Model Order Reduction via a Generalized POD Approach

Manuel Baumann* Jan Heiland†

August 17, 2012

Contents

1 Introduction **2**

2 Notation **2**

3 Standard POD **3**

4 FEM-POD **3**

5 Model Reduction and Error Analysis **6**

6 Numerical Examples **7**

7 Conclusion and Outlook **11**

*The work of M. Baumann has been carried out as a summer project at TU Berlin within the Erasmus Mundus Master's Programme *Computer Simulations for Science and Engineering (COSSE)*. mbaumann@math.tu-berlin.de

†TU Berlin, Institute for Mathematics, heiland@math.tu-berlin.de

1 Introduction

Model order reduction (MOR) is a technique to reduce the computational complexity of large-scale dynamical systems by lower dimensional approximations that capture most of the dynamical behavior of the full order system. When the considered dynamical system is nonlinear, *reduced basis* algorithms are a method of choice, cf. [MQR12]. Therein, the reduced system is obtained by a Galerkin projection onto the subspace spanned by the reduced basis which is assumed to capture the essential dynamics. The technique of determining such a reduced basis by considering snapshots of the solution trajectory and applying a singular value decomposition to detect the dominant directions in the trajectory is widely used and often referred to as proper orthogonal decomposition (POD), principal component analysis or Karhunen-Loève decomposition.

POD is successfully applied in many technical applications. However the choice of the snapshots and, subsequently, the choice of the dominant directions make POD a fairly heuristic approach. This is reflected in the common error estimates, cf. [Vol11] that are formulated for a continuous POD and that are not suitable to control the reduction error in terms of the snapshots. In [KV01, KV03] error estimates are developed that quantify the error at the snapshot instances. The authors point out that the estimates are not in the standard format used for finite elements, spectral or finite difference approximations. Since in the classical POD the snapshots are not embedded in the considered function space as L^p or $\mathcal{C}$, the approximation properties cannot be established using standard approximation results.

The goal of this work is to derive estimates that quantify the approximation error of a POD reduced model in terms of the quality and quantity of the snapshots and the subsequent reduction via the POD. Thereto we extend the notion of snapshots from singular time instances $y(t_j)$, that can be interpreted as a testing $\langle y, \delta_{t_j} \rangle$ of the trajectory y against a delta impulse δ_{t_j}, to more general test functions. In this framework it is possible to quantify the approximation of the snapshots in the considered function spaces. Also, since a general test-function may capture more information on y than a delta impulse, we think, that in practise the extended POD may lead to better approximations, as is illustrated by a numerical example.

We want to stress that our proposed method is not inferior to the classical POD in terms of memory requirement for the snapshot matrix. Furthermore, we consider the numerical effort of obtaining the snapshot coefficients not necessarily higher. The possible advantage of capturing nonlocal information by nonlocal test functions may however lead to smoothing out of relevant information. This has to be met by properly choosing the time scale of the test functions.

The investigation of a generalized POD was motivated by the observation that a singular value decomposition (SVD) of a discrete linear input/output (I/O) map, as proposed in [Sch07], can be interpreted as the computation of a POD basis.

2 Notation

Our following considerations will deal with the semi-linear initial value problem

$$\dot{y}(t) = Ay(t) + f(t, y(t)), \quad t \in (0, T], \tag{1}$$

$$y(0) = y_0, \tag{2}$$

with $f : [0, T] \times \mathbb{R}^n \to \mathbb{R}^n$, $A \in \mathbb{R}^{n,n}$ is a constant matrix and a given initial condition $y_0 \in \mathbb{R}^n$. The solution to (1)-(2) is, thus, given by a function $y : [0, T] \times \mathbb{R}^n \to \mathbb{R}^n$.

An overview of the used notations is given in the following table:

$\langle y, \nu \rangle$	scalar product in time
$[0, T]$	considered time interval
$\mathbb{R}^n$	state space
m	number of snapshots/measurements
$P_r \in \mathbb{R}^{n,n}$	projector of rank $r < n$

3 Standard POD

Suppose the solution trajectory is known, we seek for a projection $P_r : \mathbb{R}^n \to \mathbb{R}^n$ of fixed rank $r \ll n$, such that minimizes the total error

$$\int_0^T \|y(t) - P_r y(t)\|^2 \, dt. \tag{3}$$

According to [Row05], the optimal projector in (3) can be found by first introducing the $n \times n$ matrix

$$R = \int_0^T y(t)y(t)^* \, dt,$$

and then compute the eigenvectors and eigenvalues of R, given by

$$R\varphi_k = \lambda_k \varphi_k, \quad \lambda_1 \geq ... \geq \lambda_n \geq 0. \tag{4}$$

Since R is symmetric and positive-semidefinite, all eigenvalues λ_k are real and nonnegative and the eigenvectors $\{\varphi_1, ..., \varphi_n\}$ form an orthonormal basis of $\mathbb{R}^n$. The main result of POD is that the optimal r-dimensional subspace is spanned by the first r eigenvectors, called *POD modes*, and the optimal projector is given by

$$P_r = \sum_{k=1}^{r} \varphi_k \varphi_k^*. \tag{5}$$

For such a POD basis $\{\varphi_i\}_{i=1}^r$, the projection error is given by the sum of the truncated eigenvalues, cf. [Vol11],

$$\int_0^T \|y(t) - P_r y(t)\|^2 \, dt = \sum_{i=r+1}^{n} \lambda_i.$$

When the solution is only available at discrete time instances $y(t_1), ..., y(t_m)$, the n-dimensional eigenvalue problem (4) can be reduced by approximation of the operator R

$$R \approx \sum_{j=1}^{m} \tau_j y(t_j) y(t_j)^* = XX^*,$$

where τ_j are weighting factors which belong to the numerical integration method and $X := [\sqrt{\tau_1} y(t_1) ... \sqrt{\tau_m} y(t_m)]$. The eigenvalue problem

$$X^* X u_k = \lambda_k u_k, \quad u_k \in \mathbb{R}^m,$$

is then a problem of size $m \times m$ with eigenvalues λ_k which are the same as in (4) and POD modes given by $\varphi_k = Xu_k / \sqrt{\tau_k}$. Note that the POD modes can also be obtained by computing the first r left singular vectors of the snapshots matrix

$$Y = \begin{bmatrix} y_1(t_1) & \dots & y_1(t_m) \\ \vdots & \ddots & \vdots \\ y_n(t_1) & \dots & y_n(t_m) \end{bmatrix} \in \mathbb{R}^{n,m}, \tag{6}$$

which might be computed much faster if the number of snapshots m is small compared to the problem dimension n.

4 FEM-POD

As mentioned in the introduction, the main idea behind the presented extension of the standard POD approach is based on the observation that the entries of the snapshot matrix (6) can be interpreted as a testing against the appropriate delta impulse:

$$y_i(t_j) = \langle y_i, \delta_{t_j} \rangle_{L^2(0,T)}. \tag{7}$$

The proposed method projects the solution of the considered dynamical system onto a lower dimensional subspace. An improvement is expected from the global testing against a generalized set of test functions different from the delta impulse. This procedure also justifies the name *FEM-POD*.

SVD of a generalized measurement matrix

Consider the m-dimensional subspace $\mathbb{D} \subset L^2(0,T)$ spanned by the basis vectors $\{\nu_1, ..., \nu_m\}$. A projection of the solution y onto $\mathbb{D}^n$ is given by

$$y_D = \begin{bmatrix} a_{11} & \dots & a_{1m} \\ \vdots & \ddots & \dots \\ a_{n1} & \dots & a_{nm} \end{bmatrix} \begin{bmatrix} \nu_1 \\ \vdots \\ \nu_m \end{bmatrix}, \tag{8}$$

with coefficients that are obtained from the canonical projection

$$\langle y_i, \nu_k \rangle = \langle \sum_{j=1}^{m} a_{ij} \nu_j, \nu_k \rangle, \quad k = 1, ..., m, \quad i \in \{1, ..., n\}, \tag{9}$$

which can be expressed in matrix form

$$\begin{bmatrix} \langle y_i, \nu_1 \rangle \\ \vdots \\ \langle y_i, \nu_m \rangle \end{bmatrix} = M_D \mathbf{a}_i^* \quad \Leftrightarrow \quad \mathbf{a}_i = \begin{bmatrix} \langle y_i, \nu_1 \rangle & \dots & \langle y_i, \nu_m \rangle \end{bmatrix} M_D^{-1},$$

where the mass matrix M_D is given via

$$M_D = \begin{bmatrix} \langle \nu_1, \nu_1 \rangle & \dots & \langle \nu_1, \nu_m \rangle \\ \vdots & \ddots & \vdots \\ \langle \nu_m, \nu_1 \rangle & \dots & \langle \nu_m, \nu_m \rangle \end{bmatrix} \in \mathbb{R}^{m,m}. \tag{10}$$

Stacking the coefficients of all n components of the solution into a matrix, one obtains the generalized measurement matrix Y_G as

$$Y_G = \begin{bmatrix} \langle y_1, \nu_1 \rangle & \dots & \langle y_1, \nu_m \rangle \\ \vdots & \ddots & \vdots \\ \langle y_n, \nu_1 \rangle & \dots & \langle y_n, \nu_m \rangle \end{bmatrix} \in \mathbb{R}^{n,m}. \tag{11}$$

Thus, the approximation y_D can be computed as a product of the inverse of the mass matrix and the newly introduced matrix of measurements:

$$y_D = Y_G M_D^{-1} \begin{bmatrix} \nu_1 \\ \vdots \\ \nu_m \end{bmatrix} =: Y_G M_D^{-1} \nu.$$

Next, one is interested in finding the optimal projector of rank r in order to formulate the Galerkin projection and to derive the reduced system similar to 15. Therefore, the operator R is formed from (10) and (11), as the following calculation shows:

$$\begin{aligned} R &= \int_0^T y_D y_D^* \, dt = \int_0^T Y_G M_D^{-1} \nu(t) \nu(t)^* M_D^{-1} Y_G^* \, dt \\ &= Y_G M_D^{-1} \underbrace{\int_0^T \nu(t) \nu(t)^* \, dt}_{=M_D} M_D^{-1} Y_G^* = Y_G M_D^{-1} Y_G^*. \end{aligned} \tag{12}$$

Again, the first r eigenvectors of R form an optimal projector of rank r and the reduced system can be obtained analogously to (14)-(15).

Because of the special structure of the matrix R, these eigenvectors are computed by an SVD of the following $m \times m$ matrix

$$Y_G M_D^{-1/2} = U \Sigma V^T, \tag{13}$$

where $M_D^{-1/2}$ can be calculated from the square root of the corresponding diagonalization matrix.

Note, that the second part of this method is performed in analogy to the standard POD, but with the generalized measurement matrix Y_G instead of the snapshot matrix. A numerical comparison of both approaches is presented in section 6.

Projection error

We use the L^2 norm for vector valued functions to measure y_D as

$$\|y_D\|^2 = \sum_{i=1}^{n} \|y_{D,i}\|^2_{L^2(0,T)} = \sum_{i=1}^{n} \int_0^T \|y_{D,i}(t)\|_{\mathbb{R}} dt.$$

Note, that the norm of one component of y_D can be computed by the vector norm of its coefficients, weighted by the mass matrix M_D:

$$\|y_{D,i}\|^2_{L^2(0,T)} = \int_0^T \mathbf{a}_i^* \nu(t) \nu(t)^* \mathbf{a}_i \; dt = \mathbf{a}_i^* M_D \mathbf{a}_i =: \|\mathbf{a}_i\|^2_{M_D}, \quad i \in \{1, ..., n\}$$

Thus, the L^2 norm of y_D can be expressed using the tensor product for the weighting matrix

$$\|y_D\|^2 = \|\underline{a}\|^2_{I_n \otimes M_D},$$

with $\underline{a} := [a_{11}, ..., a_{1m}, ..., a_{n1}, ..., a_{nm}]$.

With $\Phi := \begin{bmatrix}\phi_1 & \cdots & \phi_n\end{bmatrix} =: \begin{bmatrix}\Phi_r & \Phi_{n-r+1}\end{bmatrix}$ being an orthonormal matrix built-up from the eigenvectors of R as defined in (12) and $P_r = \Phi_r \Phi_r^*$, we have

$$\begin{aligned}
\|y_D - P_r y_D\|^2 &= \int_0^T \|y_D(t) - P_r y_D(t)\|_{\mathbb{R}^n}^2 \, dt \\
&= \int_0^T \|\Phi^* y_D(t) - \Phi^* P_r y_D(t)\|_{\mathbb{R}^n}^2 \, dt \\
&= \int_0^T \| \begin{bmatrix} 0 \\ \Phi_{n-r+1}^* \end{bmatrix} Y_G M_D^{-1} \begin{bmatrix} \nu_1 \\ \vdots \\ \nu_m \end{bmatrix} \|_{\mathbb{R}^n}^2 \, dt \\
&= \sum_{i=n-r+1}^{n} \int_0^T \|\phi_i^* Y_G M_D^{-1} \begin{bmatrix} \nu_1 \\ \vdots \\ \nu_m \end{bmatrix} \|_{\mathbb{R}}^2 \, dt \\
&= \sum_{i=n-r+1}^{n} \phi_i^* Y_G M_D^{-1} Y_G^* \phi_i = \sum_{i=n-r+1}^{n} \phi_i^* R \phi_i \\
&= \sum_{i=n-r+1}^{n} \lambda_i.
\end{aligned}$$

Next we will show that $P_r = \Phi_r \Phi_r^*$ is indeed optimal in the sense, that for any other projector of the form $\tilde{P}_r = \Psi_r \Psi_r *$, where the columns of $\Psi = \begin{bmatrix}\psi_1 & \cdots & \psi_n\end{bmatrix} =: \begin{bmatrix}\Psi_r & \Psi_{n-r+1}\end{bmatrix}$ form an orthonormal basis of $\mathbb{R}^n$, one has

$$\|y_D - \Psi_r \Psi_r^* y_D\| \geq \|y_D - \Phi_r \Phi_r^* y_D\|.$$

Thereto we point out that

$$\|y_D\|^2 = \|\Phi^* y_D\|^2 = \sum_{i=1}^{n} \lambda_i$$

and

$$\| \begin{bmatrix} 0 \\ \Psi_{n-r+1}^* \end{bmatrix} y_D \|^2 \text{ is minimal } \Leftrightarrow \| \begin{bmatrix} \Psi_r^* \\ 0 \end{bmatrix} y_D \|^2 \text{ is maximal}$$

if considering orthogonal matrices Ψ. Thus it suffices to show that

$$\| \begin{bmatrix} \Psi_r^* \\ 0 \end{bmatrix} y_D \|^2 \leq \| \begin{bmatrix} \Phi_r^* \\ 0 \end{bmatrix} y_D \|^2 = \sum_{i=1}^{r} \lambda_i$$

to conclude optimality of P_r. We start with $r = 1$ and leave the general case to the interested reader.

With $\Psi_1 = \psi_1 = \Phi \Phi^* \psi_1$ we have

$$\| \begin{bmatrix} \psi_1 \\ 0 \end{bmatrix} y_D \|^2 = \psi_1^* \Phi \Phi^* R \Phi \Phi^* \psi_1 = \tilde{\psi}_1^* \begin{bmatrix} \lambda_1 & & \\ & \ddots & \\ & & \lambda_n \end{bmatrix} \tilde{\psi}_1 \leq \lambda_1 \tilde{\psi}_1^* I \tilde{\psi}_1 = \lambda_1,$$

since for unitary ψ_1 also $\tilde{\psi}_1 := \Phi^* \psi_1$ is unitary.

5 Model Reduction and Error Analysis

Model reduction via Galerkin projection

Let $\Phi_r = [\varphi_1, ..., \varphi_r]$ be the matrix which contains the r POD modes, either obtained by an SVD of the classical snapshot matrix or by the FEM-POD method. The solution to the reduced system

is assumed in the subspace span$\{\varphi_1, ..., \varphi_r\}$ and is represented via its r coefficients $\alpha_1, ..., \alpha_r$:

$$y^r(t) = \sum_{j=1}^{r} a_j(t)\varphi_j \approx y(t). \tag{14}$$

In order to determine these coefficients, a Galerkin projection is applied to the system (1). Then, the reduced system reads

$$\dot{\alpha} = \tilde{A}\alpha + \Phi_r^* f(y^r), \quad \text{with } \tilde{A} := \Phi_r^* A \Phi_r,\ \alpha := [\alpha_1, ..., \alpha_r]^T, \tag{15}$$

which is a closed system of only r equations.

We want to estimate the error between the actual solution y and the solution of the reduced system y^r. Thereto we use the decomposition

$$y - y^r = y - y_D + y_D - P_r y + P_r y - y_D^r + y_D^r - y^r, \tag{16}$$

where $y_D^r =: P_D y^r$ is the image of y^r if projected onto $\mathbb{D}$ via (9). We estimate the partial errors:

- $y - y_D = [I - P_D]y$ and $y_D^r - y^r = -[I - P_D]y^r$ are given by the interpolation error that comes with the choice of $\mathbb{D}$. For example, if one uses piecewise linear functions on a grid of size h one has for sufficiently smooth y that $\|[I - P_D]y\| \leq Ch^2$ for a constant $C = C(y)$ and as $h \to 0$.
- $y_D - P_r y_D$ is the projection error as computed above
- Since the projections P_r and P_D commute we can write

$$P_r y_D - y_D^r = P_D[P_r y - y^r], \tag{17}$$

  which is the error of the continuous POD, as treated in Volkwein [Vol11], projected to $\mathbb{D}$.

If we don't take any further action, we can quantify the error using the estimates of Volkwein. The additional interpolation errors account for the comparison of the snapshots with the continuous solutions which was not possible in the classical POD approach.

However we still want to improve the error bounds by considering that $P_r y - y^r$ is projected to a finite dimensional space and by decomposing again

$$P_r y - y^r = P_r y - Q_r y + Q_r y - y^r, \tag{18}$$

where Q_r is the so called Ritz- or elliptic projection that plays a role in the error estimation of Ritz-Galerkin approximations of parabolic and semilinear PDEs.

6 Numerical Examples

The presented numerical example was taken from [Cha11]. Therein, the author considers the FitzHugh-Nagumo model, a system of partial differential equations. The PDEs are discretized in space using the method of finite elements and, thus, approximated by an ODE which fits in the setup of (1) since the (linear) differential operators are represented by the matrix A and nonlinearities in the right-hand side arise as well.

The FitzHugh-Nagumo model

The FitzHugh-Nagumo (F-N) equations are a system of two coupled, non-linear partial differential equations which arises in neuron modeling. The variables

$$v : [0, L] \times [0, T] \to \mathbb{R},$$
$$w : [0, L] \times [0, T] \to \mathbb{R}$$

are voltage and recovery voltage, respectively.

According to [CJ01], the F-N system is given by (19)-(22). For $x \in (0, L), t > 0$,

$$\varepsilon v_t = -\varepsilon^2 v_{xx} + f(v) - w + c, \tag{19}$$
$$w_t = bv - \gamma w + c, \tag{20}$$

with nonlinear function $f(v) = v(v - 0.1)(1 - v)$ and initial and boundary conditions

$$v(x, 0) = w(x, 0) = 0, \quad x \in [0, L], \tag{21}$$
$$v_x(0, t) = -i_0(t), v_x(L, t) = 0, \quad t \geq 0. \tag{22}$$

The stimulus on the left boundary is given by $i_0(t) = 50000t^3 \exp(-15t)$. The set of parameters for the numerical simulation is defined in Table 1.

Some words on the numerical simulation

The discretization in space has been obtained by N equidistantly distributed grid points $\{0 = x_1, ..., x_N = L\}$. Then, the vector of unknowns $\mathbf{y} := \begin{bmatrix} \mathbf{v} \\ \mathbf{w} \end{bmatrix}$ is of dimension $2N$. A finite differences approach in space leads to a system of ODEs of the following form

$$E\dot{\mathbf{y}} = A\mathbf{y} + \mathbf{g}(t) + \mathbf{c} + \mathbf{F}(\mathbf{y}), \quad A := \begin{bmatrix} \frac{\varepsilon}{\Delta x} K_N & -\frac{1}{\varepsilon} I_N \\ bI_N & -\gamma I_N \end{bmatrix}, \tag{23}$$

where K_N is the one-dimensional discrete Laplacian, I_N is the identity of size $N \times N$ and the boundary conditions (21) are represented in the vector $\mathbf{g}(t)$. Furthermore, $\mathbf{c}$ is a constant vector, $E = \text{diag}[\varepsilon, ..., \varepsilon, 1, ..., 1] \in \mathbb{R}^{2N,2N}$ and $\mathbf{F}(\mathbf{y})$ contains the nonlinearity.

Since E is invertible, the system fits in the setup of (1)

$$\begin{aligned} \dot{\mathbf{y}} &= E^{-1}(A\mathbf{y} + \mathbf{g}(t) + \mathbf{c} + \mathbf{F}(\mathbf{y})) \\ &= \tilde{A}\mathbf{y} + \tilde{\mathbf{F}}(t, \mathbf{y}(t)), \quad \text{with } \tilde{A} := E^{-1}A, \ \tilde{\mathbf{F}}(t, \mathbf{y}(t)) := E^{-1}(\mathbf{g}(t) + \mathbf{c} + \mathbf{F}(\mathbf{y})) \end{aligned}$$

and the ODE has been solved by the MATLAB built-in function `ode15s` together with the suitable options.

L	T	ε	b	γ	c
1	8	0.015	0.5	2	0.05

Table 1: Parameter configuration.

The v-component of the numerical solution of the full order system is shown in Figure 5.

The standard POD approach

The reduced order model (ROM) is obtained from $m = 9$ snapshots taken at equidistant points in $[0, T]$. A plot of the singular values of the snapshot matrix (6) is presented in Figure 1. Interpreting the singular values as measures for the system's energy, more than 99% of it is captured when only considering the first three POD modes, cf. Table 2. Thus, the reduced model is constructed by a Galerkin projection as described in (15) with $r = 3$.

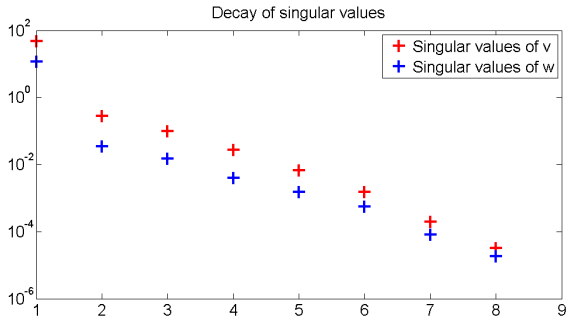

Figure 1: Decay of the singular values based on 9 snapshots taken at equidistant time instances.

FEM-POD with piecewise linear, hierarchical basis functions

To obtain a FEM-POD reduced system, one needs a basis of the considered subspace $\mathbb{D}$. Here, we chose the subspace of piecewise linear functions on $[0, T]$ with a hierarchical basis as illustrated in Figure 2. To comply with the POD reduction above in terms of memory requirement for the measurement matrix, the first $m = 9$ functions $\{\nu_1, ..., \nu_9\}$ were used to construct $\mathbb{D}$ and to form the matrices M_D and Y_G.

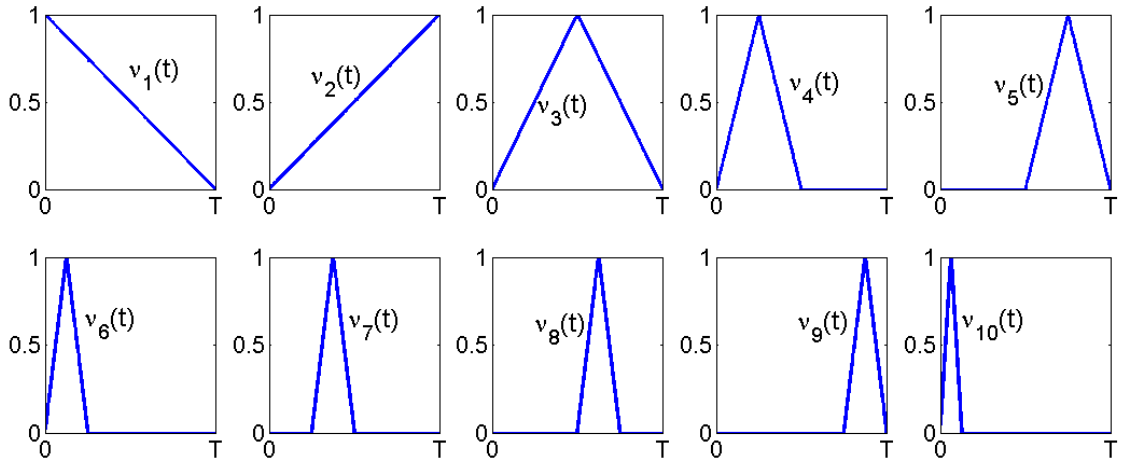

Figure 2: The first ten basis function $\nu_1, ..., \nu_{10}$ defined for $t \in [0, T]$.

The decay of the singular values of the considered matrix (13) is shown in Figure 3. Again, the first three singular values capture more than 99% of the energy (see Table 2).

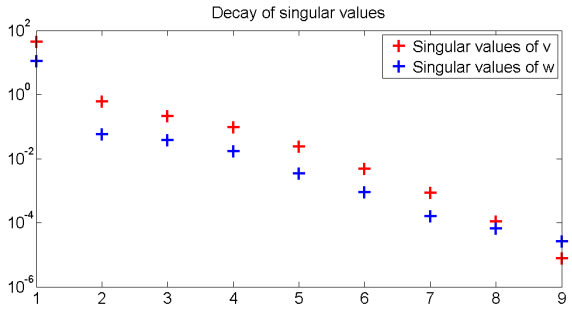

Figure 3: Decay of the singular values of the matrix $Y_G M_D^{-1/2}$.

Again, the corresponding reduced system that takes the 3 dominant directions as ansatz functions.

Comparison of the Reduced Models

The difference of the solutions of the reduced systems to the full order solution is plotted in Figure 4. Moreover, the global error is measured in the L^2 norm and in the maximum norm, see Table 2.

The FEM-POD reduced system outperforms the system of the same size obtained by the standard approach both in the discrete L^2 and in the maximum norm. In particular the peak at the first amplitude is computed more accurate by the generalized FEM-POD procedure, see Figure 5.

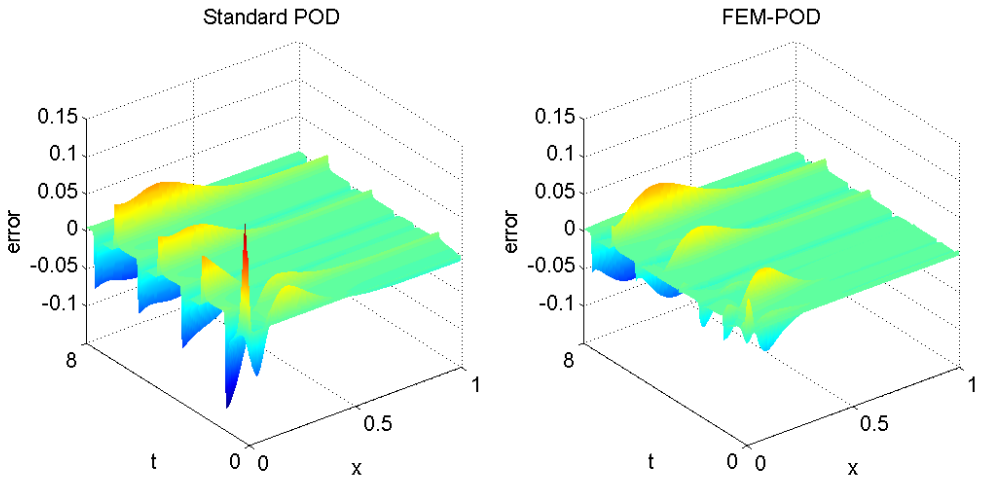

Figure 4: Global error of the reduced solution for Standard POD (left) and FEM-POD (right).

	Standard POD	FEM-POD
$\sum_{i=1}^{r} \sigma_i / \sum_{i=1}^{m} \sigma_i$	0.9992	0.9973
error in $\|\cdot\|_{L^2([0,T]\times[0,L])}$	7.6965e-005	6.0294e-005
error in $\|\cdot\|_{\infty}$	0.1436	0.0775

Table 2: Overview of the model reduction error.

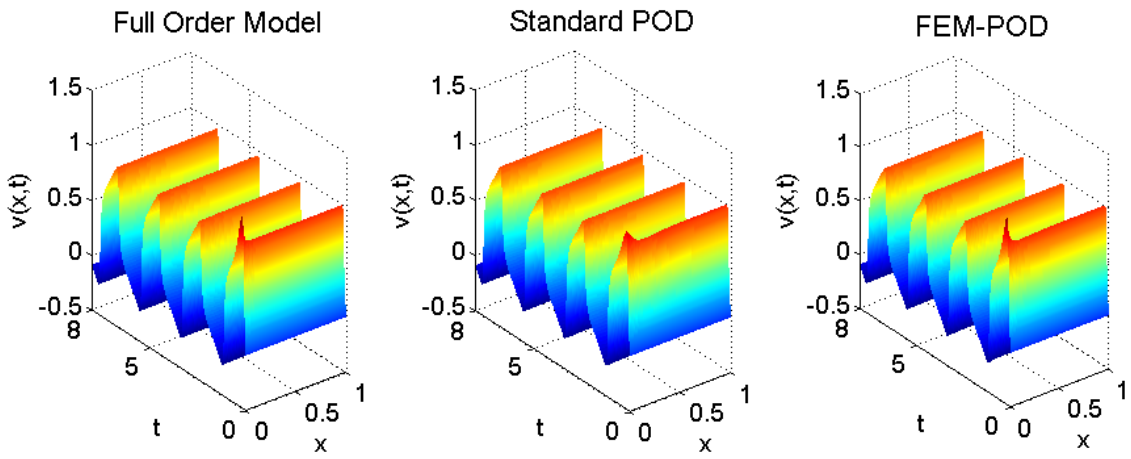

Figure 5: Full order solution (left) together with the reduced model solutions in the case of standard POD (middle) and FEM-POD (right).

7 Conclusion and Outlook

The main achievement of this work is the development and testing of a generalization of the well-known POD method for model order reduction of nonlinear dynamical systems. In section 4, the so-called FEM-POD method has been derived based on a testing of the trajectory y against more general functions than a delta impulse. By this procedure, a matrix called the *matrix of measurements* Y_G has been constructed and the reduced system has been obtained by a Galerkin projection built from the first r singular vectors of the product of Y_G with the mass matrix.

A numerical tests has shown that the solution to the reduced system captures the dynamics of the full order system very well. Here, the newly developed method showed a significant improvement to the standard POD method when measuring the error in the maximum norm.

Furthermore, we think, that on more complex spatial dynamics the FEM-POD will perform even better, as in the considered example, where the POD reduction of order 3 is already quite, there is little space for improvements.

Thus, a future task is the investigation of more involved dynamics. Also, we will use the function space setting to really develop new error estimates for the FEM-POD-Galerkin approximation.

References

[Cha11] S. Chaturantabut. *Nonlinear Model Reduction via Discrete Empirical Interpolation.* PhD thesis, Rice University, 2011.

[CJ01] S. J. Cox and L. Ji. Discerning ionic currents and their kinetics from input impedance data. *Bulletin of Mathematical Biology*, 63:909–932, 2001.

[KV01] K. Kunisch and S. Volkwein. Galerkin proper orthogonal decomposition methods for parabolic problems. *Numerische Mathematik*, 90:117–148, 2001. 10.1007/s002110100282.

[KV03] K. Kunisch and S. Volkwein. Galerkin proper orthogonal decomposition methods for a general equation in fluid dynamics. *SIAM Journal on Numerical Analysis*, 40(2):pp. 492–515, 2003.

[MQR12] A. Manzoni, A. Quarteroni, and G. Rozza. Computational reduction for parametrized PDEs: Strategies and applications. *Milan Journal of Mathematics*, pages 1–27, 2012. 10.1007/s00032-012-0182-y.

[Row05] C. W. Rowley. Model reduction for fluids, using balanced proper orthogonal decomposition. *Int. J. on Bifurcation and Chaos*, 2005.

[Sch07] M. Schmidt. *Systematic Discretization of Input/Output Maps and other Contributions to the Control of Distributed Parameter Systems.* PhD thesis, TU Berlin, Fakultät Mathematik, Berlin, Germany, 2007.

[Vol11] S. Volkwein. Model reduction using proper orthogonal decomposition. Lecture notes, 2011.